DRAFT VERSION FEBRUARY 6, 2013
Preprint typeset using LaTeX style emulateapj v. 2/19/04

ASTEROSEISMIC CLASSIFICATION OF STELLAR POPULATIONS AMONG 13 000 RED GIANTS OBSERVED BY *KEPLER*

DENNIS STELLO,[1,2] DANIEL HUBER,[3] TIMOTHY R. BEDDING,[1,2] OTHMAN BENOMAR,[1,2] LARS BILDSTEN,[4,5] YVONNE P. ELSWORTH,[6] RONALD L. GILLILAND,[7] BENOÎT MOSSER,[8] BILL PAXTON,[4] TIMOTHY R. WHITE[1,2]

Draft version February 6, 2013

ABSTRACT

Of the more than 150 000 targets followed by the *Kepler Mission*, about 10% were selected as red giants. Due to their high scientific value, in particular for Galaxy population studies and stellar structure and evolution, their *Kepler* light curves were made public in late 2011. More than 13 000 (over 85%) of these stars show intrinsic flux variability caused by solar-like oscillations making them ideal for large scale asteroseismic investigations. We automatically extracted individual frequencies and measured the period spacings of the dipole modes in nearly every red giant. These measurements naturally classify the stars into various populations, such as the red giant branch, the low-mass ($M/\mathrm{M}_\odot \lesssim 1.8$) helium-core-burning red clump, and the higher-mass ($M/\mathrm{M}_\odot \gtrsim 1.8$) secondary clump. The period spacings also reveal that a large fraction of the stars show rotationally induced frequency splittings. This sample of stars will undoubtedly provide an extremely valuable source for studying the stellar population in the direction of the *Kepler* field, in particular when combined with complementary spectroscopic surveys.

Subject headings: stars: interiors — stars: oscillations — techniques: photometric

1. INTRODUCTION

We have seen dramatic progress in the asteroseismology of red giant stars in recent years, driven by the quantum leap in data quality and quantity arising from the space missions CoRoT (Baglin et al. 2006) and *Kepler* (Koch et al. 2010; Gilliland et al. 2010). We can now start using large samples of stars to study stellar evolution in different populations within the Galaxy to a degree that has not been possible before.

For about a decade it has been evident that red giants show oscillations excited by near-surface convection like in the Sun (Frandsen et al. 2002), known as solar-like oscillations. This sparked hope that one could obtain rich information about the interior structure of red giant stars, analogous to what global helioseismology had taught us about the Sun (Christensen-Dalsgaard 2002). However, only recently was it demonstrated that the frequency spectra of red giants comprised both radial and non radial modes (de Ridder et al. 2009), whose frequencies, $\nu_{n,l}$, largely followed the asymptotic relation for high-order, n, and low-degree, l, acoustic (p) modes (Vandakurov 1967; Tassoul 1980; Gough 1986) as for the Sun,

$$\nu_{n,l} \simeq \Delta\nu(n + l/2 + \epsilon) - \delta\nu_{0,l}\,. \quad (1)$$

Here, ϵ is the offset from zero of the fundamental radial mode in units of the large separation, $\Delta\nu$, which is the frequency shift of consecutive overtone modes of the same degree, and $\delta\nu_{0,l}$ is the small separation of non-radial modes relative to radial modes following the notation of (Bedding 2011). It was subsequently shown (Bedding et al. 2010; Huber et al. 2010; Mosser et al. 2011b) that the frequency spectra of the p modes in red giants are essentially similar under a simple scaling, which implies that the stars are largely homologous.

In addition to the regular, and largely scalable, frequency pattern of the p modes, red giants show a more complex pattern arising from large numbers of mixed modes, most pronounced for dipole, $l = 1$, modes (Bedding et al. 2010). These mixed modes are the result of coupling between the many dipole gravity (g) modes in the core, which are approximately equally (and closely) spaced in period, and the more widely spaced dipole p modes in the envelope, which are approximately equally spaced in frequency (Dupret et al. 2009). While the coupling between p- and g-modes shifts the frequencies from their equal spacing, a process known as mode bumping, the period spacing of the mixed modes still is a proxy for the intrinsic period spacing of the g modes in the core (Beck et al. 2011). A detailed study of the difference between the period spacing of uncoupled g-modes and that of the mixed modes was conducted by Mosser et al. (2012a).

Due to their partial g-mode nature, the mixed modes offer a 'window' into the structure of the stellar cores. Bedding et al. (2011) showed that their period spacing distinguish red giant branch stars, burning only hydrogen in the shell, from red clump stars that also burn helium in their cores. More recently, Beck et al. (2012) demonstrated that the mixed modes probe the internal differential rotation of red giants, enabling investigations into the transport of angular momentum as stars 'climb' the red giant branch (Mosser et al. 2012b).

The potential for obtaining new results on red giants was recently boosted by the public release of over two years of *Kepler* data for about 15 000 stars classified as giants in the *Kepler* Input Catalog – providing an order of magnitude more stars with such long time series than has previously been available through the Kepler Asteroseismic Science Consortium. Initial analyses were performed by Hekker et al. (2011) who measured $\Delta\nu$ and the location of the maximum oscilla-

[1] Sydney Institute for Astronomy (SIfA), School of Physics, University of Sydney, NSW 2006, Australia
[2] Stellar Astrophysics Centre, Department of Physics and Astronomy, Aarhus University, DK-8000 Aarhus C, Denmark
[3] NASA Ames Research Center, Moffett Field, CA 94035, USA
[4] Kavli Institute for Theoretical Physics, University of California, Santa Barbara, CA 93106, USA
[5] Department of Physics, University of California, Santa Barbara, CA 93106, USA
[6] School of Physics and Astronomy, University of Birmingham, Edgbaston, Birmingham B15 2TT, UK
[7] Center for Exoplanets and Habitable Worlds, The Pennsylvania State University, University Park, PA 16802, USA
[8] LESIA, CNRS, Université Pierre et Marie Curie, Université Denis Diderot, Observatoire de Paris, 92195 Meudon, France

tion power, $\nu_{\rm max}$, of roughly 11 000 of these red giants based on the first 43 days of *Kepler* data.

Here, we report a search for oscillations in this much longer data set in order to perform 'ensemble peak-bagging' – extracting oscillation frequencies on large numbers of stars. From these we measure characteristic separations of the modes in frequency and period, which we analyze to identify different stellar populations and demonstrate the potential for follow-up investigations of this extremely valuable stellar sample.

2. DATA ANALYSIS

Our initial data set comprised photometric time series of 15 261 stars observed by *Kepler* from 2009 May 2 to 2011 March 14 (observing quarters 0–8) in the long-cadence mode ($\delta t = 29.4244$ minutes), with a median time span of just below two years. Most of these stars are expected to be red giants (Hekker et al. 2011). The large number of stars in our sample calls for an automated approach to the analysis, which we describe below.

2.1. *Measuring global seismic properties*

We have used simple aperture photometry (SAP) data for our analysis (Jenkins et al. 2010), downloaded from the MAST database[9]. Jumps in each time series (e.g. across quarterly gaps) were corrected by fitting and removing a linear regression to 5-day light curve segments before and after each gap. Remaining slow instrumental trends were then removed by subtracting a smoothed version of the light curve that was calculated by applying a boxcar filter with a width of 10 days. The high-pass-filtered light curves were then used to calculate a frequency spectrum. This was analyzed with an automated pipeline (Huber et al. 2009) to detect the presence of solar-like oscillations. The results from the pipeline were verified by visual inspection of its graphical output of each star, and a few percent of the stars were discarded in this process because the pipeline results were deemed incorrect. Oscillations were detected in 13 412 red giant stars. We found a similar number (13 182) when using the method described in Mosser & Appourchaux (2009). Hence, for $\sim 2\,000$ stars, predominantly low and high $\log\, g$ giants, we 'missed' the oscillations because of the high-pass filter and the limits set by the Nyquist frequency of the data, respectively. For each star, the analysis provided a frequency spectrum corrected for the stellar granulation signal, as well as measurement of $\nu_{\rm max}$ and $\Delta\nu$ (Figure 1(a)).

2.2. *Extracting oscillation mode frequencies*

Using an approach similar to Bedding et al. (2011), we smoothed the frequency spectra and measured the frequency of each peak reaching above three times the noise level within $\pm 5\Delta\nu$ of $\nu_{\rm max}$. A smoothing width of about 0.1–0.2μHz provided a good compromise, enabling the detection of closely spaced narrow peaks from long lived modes while keeping the number of spurious detections low around broad peaks arising from single short lived modes (Figure 1(b–d)).

We associated the frequencies, ν, with radial or quadrupole ($l = 0$ and 2) modes if $\epsilon - 0.3 < \nu/\Delta\nu \bmod 1 < \epsilon + 0.1$, where ϵ was derived using the $\Delta\nu$-ϵ relation fitted to red giant branch stars by Corsaro et al. (2012) based on the formulation by Mosser et al. (2011b) (Figure 1(b–d), shaded regions).

[9] http://archive.stsci.edu/kepler/

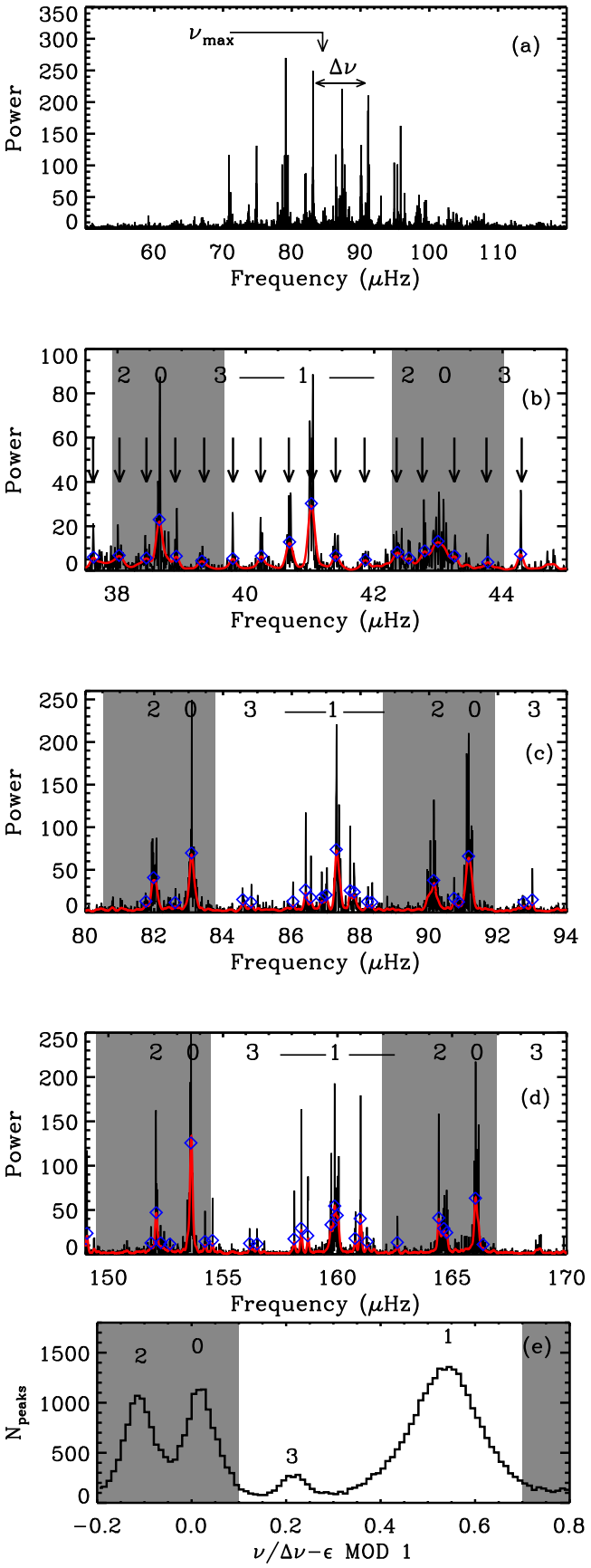

FIG. 1.— (a) Frequency spectrum (noise normalized power) of a red giant branch star, with $\nu_{\rm max}$ and $\Delta\nu$ indicated. (b) Small region of spectrum of a red clump star. Spherical degrees of the modes are indicated. Extracted frequencies (blue diamonds) are found as the peaks of the smoothed spectrum (red curve). Black arrows show the location of the dipole modes apparent by visual inspection. All frequencies within the gray shaded regions are however assigned as radial and quadrupole modes in our automatic approach. (c) Same as panel (b), but for a red giant branch star of high inclination angle showing rotationally split dipole modes as close doublets. (d) Same as panel (c) but

The remaining frequencies were associated with dipole modes ($l = 1$), assuming negligible contamination from $l = 3$ modes (panel (e)). To ensure robust results, we discarded stars with fewer than five detected dipole modes overall. There were 13 031 stars that passed this criterion.

2.3. *Measuring period spacings*

For each star, we calculated the pairwise period spacings, ΔP, between adjacent dipole modes, hence providing at least four spacings per star and usually many more. We plot these versus $\Delta\nu$ in Figure 2(a). In this figure we show the ΔP regime that is populated by red giant branch (first ascent) stars (below about 100 s – see Bedding et al. 2011). We find a remarkably clear upper envelope of the ΔP distribution in the range $6 < \Delta\nu/\mu\mathrm{Hz} < 16$ at values of roughly ΔP= 70–90 s, which we interpret as a signature of the 'true' g-mode period spacing of dipole modes.

To confirm this, we show the asymptotic g-mode period spacing for dipole modes, $\Delta P_g = \sqrt{2}\pi^2(\int N/rdr)^{-1}$, where N is the buoyancy frequency integrated over the radius, along a stellar model track representative for the typical stellar masses in our sample of stars (see Section 3). This is the period spacing of the g modes if they did not couple with the p modes. The alignment between ΔP_g from the model and the upper envelope of the observed ΔP is striking. The sharp edge of this upper envelope, and the fact that all tracks of representative masses fall almost on top of each other in this region (Section 3; see also Bedding et al. 2011; White et al. 2011; Mosser et al. 2012a), is strong evidence that many of the detected dipole modes are essentially separated by the true g-mode spacing, which is now directly measurable for a significant fraction of stars. In order words, these modes resemble almost pure g-modes (see example in Figure 1b). Except for some special cases, we have previously only been able to infer the true g-mode spacing when making certain assumptions about the coupling between p- and g-modes (Stello 2012; Mosser et al. 2012a).

In addition, the over density of data points just below the model track (Figure 2a) gives us further confidence that we are essentially detecting the true g-mode spacing directly in a large number of stars. To illustrate this point, we show in Figure 3 the period spacings of a sequence of $l = 1$ modes from a representative 1.5$\mathrm{M}_\odot$ model. The most common period spacings in the model are those close to the true g-mode period spacing, arising from the least bumped modes between the 'dips' in ΔP where the slope of the $\Delta P(\nu)$ 'curve' is close to zero. The same effect could explain the slightly higher number of modes spaced at about 50 s (as the slope of the $\Delta P(\nu)$ curve also becomes zero at the bottom of each dip). These two extremes are marked as Max(ΔP) and Min(ΔP) in Figure 2(b).

Stars at the bottom of the red giant branch with high values of $\Delta\nu$, towards the subgiants, typically show stronger coupling between p- and g-modes, and hence wider dips in the period spacing, compared to what is shown in Figure 3 (Dupret et al. 2009). In addition, their larger $\Delta\nu$ and ΔP makes their frequency spectra less dense, implying fewer modes spaced just below the true g-mode spacing. This seems to be supported by the absence of a clear over-density of points near the model track towards lower luminosity (higher $\Delta\nu$) in Figure 2(a).

Another clear feature in this diagram is a large number of points with $\Delta P \sim 10 - 30$ s. Many arise from rotationally split modes and are discussed in Section 3.2.

3. IDENTIFYING STELLAR POPULATIONS

3.1. *The ΔP-$\Delta\nu$ diagram*

To separate the stars into distinct groups, we need to assign a single representative value of ΔP to each star. The median of all period spacings per star provided an efficient and robust measure for this purpose. The absolute values of ΔP from this method is most likely somewhat different than those found using previously published methods (Bedding et al. 2011; Mosser et al. 2011a, 2012a), but for our purpose that is not of concern. We show the result of the median period spacing in Figure 4(a), which for clarity only includes modes that reach above six times the noise level (30 % of all stars). The masses indicated by color and shown as a histogram in the inset are derived from the scaling relation

$$M/\mathrm{M}_\odot \simeq (\nu_{\max}/\nu_{\max,\odot})^3(\Delta\nu/\Delta\nu_\odot)^{-4}(T_{\mathrm{eff}}/\mathrm{T}_{\mathrm{eff},\odot})^{3/2}, \quad (2)$$

which shows a relative scatter below 10% for samples of equal-mass stars (Miglio et al. 2012). This relation is derived from the scaling relations for $\Delta\nu$ and $\nu_{\max}$ (Kjeldsen & Bedding 1995). For T_{eff}, we used the values from Pinsonneault et al. (2012). We found qualitative agreement for this plot when comparing it with values derived using the method described in Mosser et al. (2011a).

To compare qualitatively with our observations, we plot ΔP_g for a grid of stellar models in Figure 4(b) using the MESA `1M_pre_ms_to_wd` test suite case (Paxton et al. 2011, 2013). In this diagram the models evolve from right to left along the red giant branch. The hook at $\Delta P \simeq 200$ s along each track is the bottom of the red giant branch. When helium ignites at the tip of the red giant branch with $\Delta\nu$ values close to zero (outside the plotted range), the tracks quickly reappear on the helium-burning ZAMS (open diamonds; known as the zero-age horizontal branch for low-metallicity stars). Although the tracks were computed through this very rapid phase, for clarity we do not show this. About 2-3 stars per 100 red clump stars are expected to be in this transition phase (Bildsten et al. 2012). Again, to simplify the plot the helium-core-burning phase is only shown from the helium-burning ZAMS until the core helium mass fraction has reached 0.14, except for the 1.0 $\mathrm{M}_\odot$ track (dark blue), which shows the evolution all the way to the early phases of the asymptotic giant branch (dashed). As core convection due to helium burning ends, ΔP drops from 190 seconds to 100 seconds in less than 1 Myr. At the point where helium is completely exhausted in the centre of the star, which happens at $\Delta P \simeq 80$ s for the 1.0 $\mathrm{M}_\odot$ track, the period spacing has been reduced back to something comparable to that of the red giant branch stars. We note that the change in ΔP as a function of mass along the helium-burning ZAMS follows quite tightly that of the helium core mass, which is lowest for $M \sim 2.4\,\mathrm{M}_\odot$ without overshooting (S. & M. 2013).

From the speed at which models move across this diagram (Figure 4b), seen by the density of filled dots, we expect most observed stars to occupy the region, of $50 < \Delta P < 90$ (red giant branch stars with $M \lesssim 1.8\,\mathrm{M}_\odot$), $200 < \Delta P < 250$ (red clump stars with $M \lesssim 1.8\,\mathrm{M}_\odot$), and $150 < \Delta P < 200$ (secondary clump stars with $M \gtrsim 1.8\,\mathrm{M}_\odot$). Although the median of our observed ΔP (panel a) is not exactly the same quantity as ΔP_g (panel b), the qualitative agreement between the models and the data is surprisingly good, and demonstrates that we can clearly separate the different stellar populations. How much the observed median ΔP deviate from ΔP_g depends on the fraction of individual period spacings that we

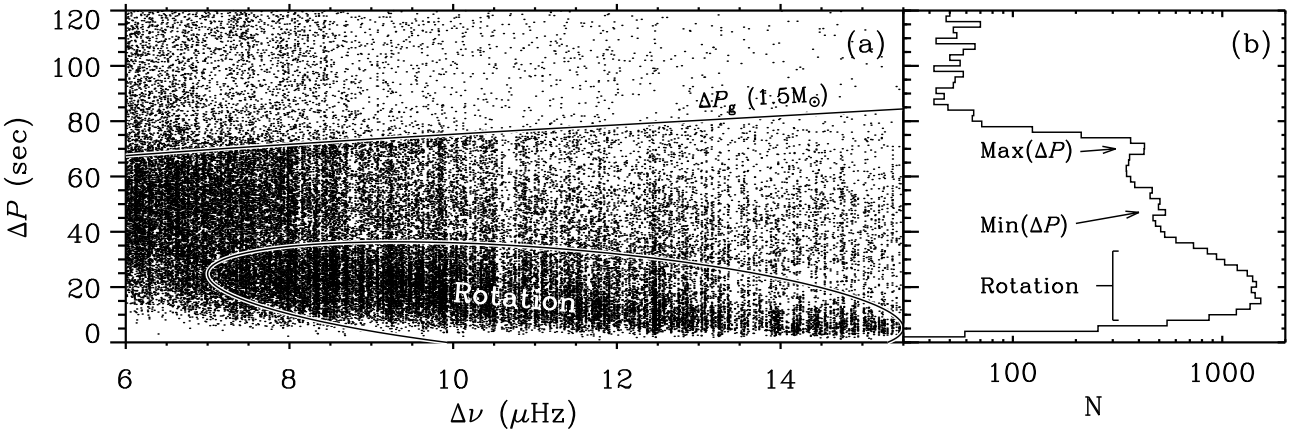

FIG. 2.— (a) ΔP versus $\Delta\nu$ for each pair of consecutive $l = 1$ modes (based on 0.1μHz smoothing of the frequency spectra). The black curve shows the asymptotic g-mode period spacing, ΔP_g, of a representative stellar model track below the red giant branch bump (see text). (b) Histogram of ΔP in the range $8 < \Delta\nu/\mu\text{Hz} < 12$.

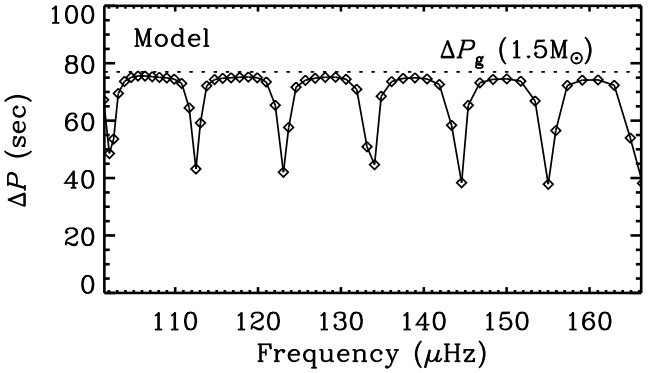

FIG. 3.— ΔP versus frequency for each pair of consecutive $l = 1$ modes (diamonds) of a red giant branch model along the 1.5M$_\odot$ track shown in Figure 2(a) with $\Delta\nu = 10.8\,\mu$Hz and $\Delta P_g = 77$ s. The dotted line marks the asymptotic period spacing.

observe within, relative to outside, the dips (Figure 3), which again depends on both the strength of the coupling between the p- and g-modes and the number of dipole modes per radial p-mode order that we detect (see e.g. Mosser et al. 2012a).

One significant difference between panels (a) and (b) is the observed low-mass (blue and green) stars in the region bracketed by $\Delta P \sim 80 - 250$ s and $\Delta\nu \sim 5 - 7\,\mu$Hz, which is unexpected when compared to the models. These stars lie in the region where Bildsten et al. (2012) predicted the helium flashing stars to be while they establish stable core burning. However, spot checks of the frequency spectra show that these stars are mainly red giant branch stars whose measured median ΔP are not representative of the actual spacing between adjacent modes caused by our limited frequency resolution. Hence, the median ΔP is artificially increased. Towards lower values of $\Delta\nu$, red giant branch stars show smaller period spacings, making it harder to resolve the individual mixed modes, which is somewhat exacerbated because we smooth the frequency spectra before we extract the frequencies. This also explains the lack of red giant branch stars with $\Delta\nu \lesssim 5\,\mu$Hz.

In Figure 4 (c) we finally look at how metallicity affects the position in the ΔP-$\Delta\nu$ diagram, in order to judge how a bias in metallicity could be introduced when selecting samples of stars from this diagram. It is quite clear that within the range of Z shown (corresponding roughly to $-0.2 < [\text{Fe/H}] < 0.2$), the models do not show any significant shift in ΔP_g, and only a slight shift in $\Delta\nu$, due to a change in mean stellar density.

3.2. *Internal rotation*

In Figure 5 we show the distribution of the observed median ΔP. Like Figure 2, it clearly shows a large fraction of stars with period spacings well below ΔP_g for red giant branch stars. Visual inspection of the frequency spectra shows that these are red giant branch stars with rotationally split dipole modes, as reported in a few stars by Beck et al. (2012) (see also the ensemble analysis by Mosser et al. (2012b)). Figures 1(c) and (d) show some typical examples of such stars. Most of the pairwise period spacings for these stars are due to the rotational splitting of the dipole modes, which is why they show up with low values of the median ΔP. As illustrated in Figure 1(c) and (d), the dipole modes split into two or three peaks depending on their angle of inclination. We see two peaks when the inclination is high (close to 90 degrees), three peaks are seen when the inclination is intermediate (∼40–60 degrees), and just one peak is seen when the star is viewed pole on (Gizon & Solanki 2003). This sample of rotating red giant branch stars provides an interesting selection for further studies into transport of angular momentum (Mosser et al. 2012b), age-rotation relations and the connection between surface and internal rotation including their angles of inclination.

4. CONCLUSION

We used a blind and fully automated approach to extract oscillation frequencies for a very large sample ($\sim 13\,000$) of red giants observed by *Kepler*. From the extracted frequencies we measured period spacings between consecutive mixed modes of angular degree $l = 1$.

For a significant number of stars we were able to directly measure period spacings of the least bumped modes, suggesting that essentially pure g modes are now observable at the stellar surface. Because the mode lifetime of the almost pure g modes is extremely long (Beck et al. 2012), we can expect these modes will show up for an increasing number of stars as the time span of the *Kepler* observation increase. This indicates great prospects to further investigate the intricate details of stellar cores in red giants.

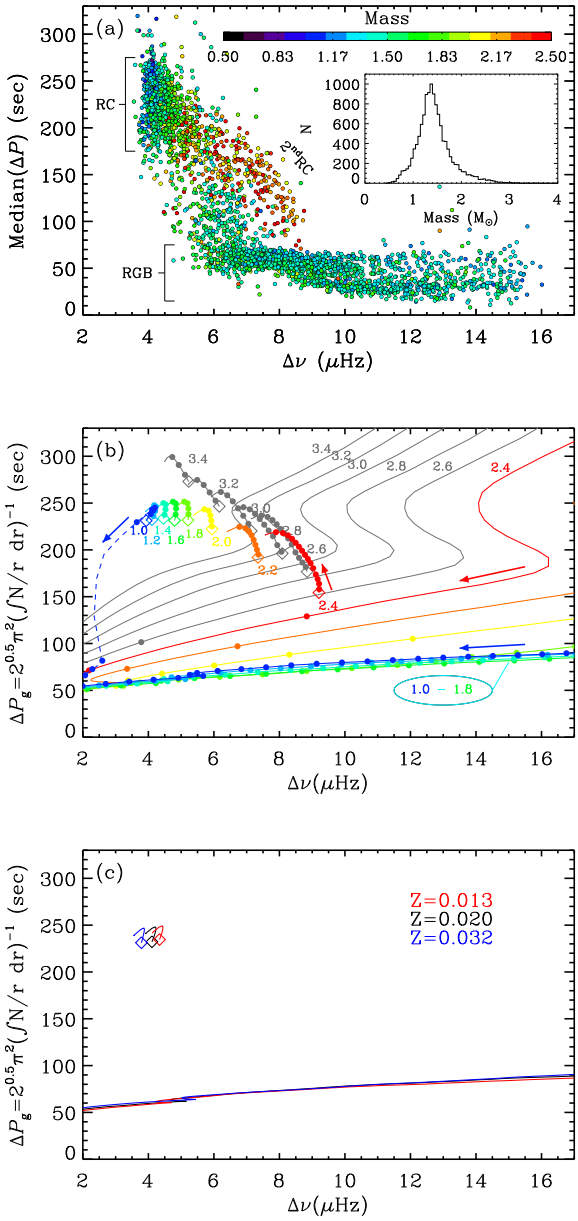

FIG. 4.— (a) Median ΔP for each star versus its $\Delta\nu$ (based on 0.2μHz smoothing of the frequency spectra). Red giant branch (RGB), red clump (RC), and secondary clump ($2^{\rm nd}$RC) stars are indicated. (b) Curves show ΔP_g from theoretical models using MESA. Filled dots are separated by 10Myrs. Arrows indicate evolutionary direction. Masses of each track are indicated and their colors follow that of panel (a). The helium-burning ZAMS is marked by diamonds for each mass. The evolution from core to shell helium burning for the 1 $M_\odot$ model is shown by the blue dashed line. (c) Same as panel (b), but for 1 $M_\odot$ tracks of three different values of the heavy element abundance.

The median of the pairwise period spacings in each star from this simple but fast approach enabled an efficient way to distinguish red giant branch and red clump stars for the majority of stars in our sample. In addition, it enabled us to separate out a large fraction of stars showing rotational splittings.

Our results demonstrate the great potential that this stellar sample holds for investigations into stellar structure and evolution, stellar populations of the Galaxy, and fundamental relationships between stellar parameters such as age, rotation, and metallicity.

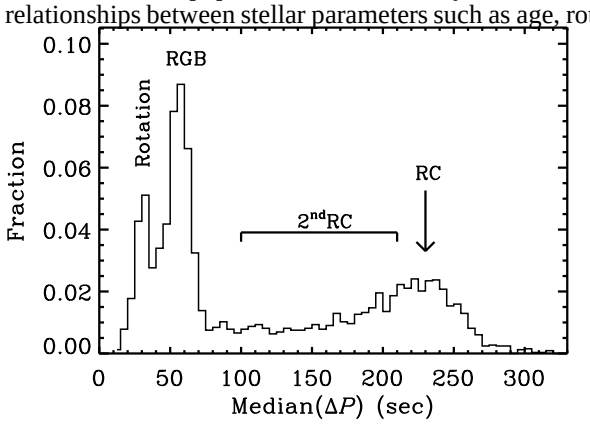

FIG. 5.— Median period spacing of stars in Figure 4(a). Different populations are indicated. The majority of stars in the range $80 \lesssim \Delta P/{\rm s} \lesssim 140$ are red giant branch stars with 'incorrectly' determined values of ΔP (see text).

Funding for this Discovery mission is provided by NASA's Science Mission Directorate. We thank the entire *Kepler* team without whom this investigation would not have been possible. This reseach has been supported by the Australian Research Council. DH is supported by an appointment to the NASA Postdoctoral Program at Ames Research Center, administered by Oak Ridge Associated Universities through a contract with NASA.

REFERENCES

Baglin, A., et al. 2006, in COSPAR, Plenary Meeting, Vol. 36, 36th COSPAR Scientific Assembly, 3749
Beck, P. G., et al. 2011, Science, 332, 205
—. 2012, Nature, 481, 55
Bedding, T. R. 2011, arXiv:1107.1723
Bedding, T. R., et al. 2010, ApJ, 713, L176
—. 2011, Nature, 471, 608
Bildsten, L., Paxton, B., Moore, K., & Macias, P. J. 2012, ApJ, 744, L6
Christensen-Dalsgaard, J. 2002, Reviews of Modern Physics, 74, 1073
Corsaro, E., et al. 2012, ApJ, 757, 190
de Ridder, J., et al. 2009, Nature, 459, 398
Dupret, M., et al. 2009, A&A, 506, 57
Frandsen, S., et al. 2002, A&A, 394, L5
Gilliland, R. L., et al. 2010, PASP, 122, 131
Gizon, L., & Solanki, S. K. 2003, ApJ, 589, 1009
Gough, D. O. 1986, in Hydrodynamic and Magnetodynamic Problems in the Sun and Stars, ed. Y. Osaki, 117
Hekker, S., et al. 2011, MNRAS, 414, 2594
Huber, D., Stello, D., Bedding, T. R., Chaplin, W. J., Arentoft, T., Quirion, P., & Kjeldsen, H. 2009, Communications in Asteroseismology, 160, 74
Huber, D., et al. 2010, ApJ, 723, 1607
Jenkins, J. M., et al. 2010, ApJ, 713, L87

Kjeldsen, H., & Bedding, T. R. 1995, A&A, 293, 87
Koch, D. G., et al. 2010, ApJ, 713, L79
Miglio, A., et al. 2012, MNRAS, 419, 2077
Mosser, B., & Appourchaux, T. 2009, A&A, 508, 877
Mosser, B., et al. 2011a, A&A, 532, A86
—. 2011b, A&A, 525, L9
—. 2012a, A&A, 540, A143
—. 2012b, A&A, 548, A10
Paxton, B., Bildsten, L., Dotter, A., Herwig, F., Lesaffre, P., & Timmes, F. 2011, ApJS, 192, 3
Paxton, B., et al. 2013, arXiv1301.0319
Pinsonneault, M. H., An, D., Molenda-Żakowicz, J., Chaplin, W. J., Metcalfe, T. S., & Bruntt, H. 2012, ApJS, 199, 30
S., C., & M., S. 2013, Old Stellar Populations: How to Study the Fossil Record of Galaxy Formation (Wiley, ISBN: 978-3-527-41076-7)
Stello, D. 2012, in Astronomical Society of the Pacific Conference Series, Vol. 462, Progress in Solar/Stellar Physics with Helio- and Asteroseismology, ed. H. Shibahashi, M. Takata, & A. E. Lynas-Gray, 200
Tassoul, M. 1980, ApJS, 43, 469
Vandakurov, Y. V. 1967, AZh, 44, 786 (English translation: Soviet Astronomy AJ, 11, 630)
White, T. R., Bedding, T. R., Stello, D., Christensen-Dalsgaard, J., Huber, D., & Kjeldsen, H. 2011, ApJ, 743, 161